Antarctic Science 7 (1): 39–50 (1995)

Current flow in the north-west Weddell Sea

MARION BARBER[1] and DAVID CRANE[2]

[1]British Antarctic Survey, Natural Environment Research Council, High Cross, Madingley Road, Cambridge, CB3 OET, UK
[2]Scott Polar Research Institute, University of Cambridge, Lensfield Road, Cambridge, CB2 1EG, UK

Abstract: Properties of the surface and bottom circulation in the north-west Weddell and south Scotia seas in the region 59–66°S, 36–46°W are examined. The bottom currents have been recorded at different heights from 5– 800 m above the seabed, and surface velocities have been obtained from the drift tracks of ARGOS buoys deployed in ice floes. The tidal regime is mixed and the power of motions at inertial frequencies is very variable and most dominant in the Scotia Sea. Flow is influenced by topography, effects of which are seen in eddy features and the damping of inertial motions in some areas. The sea ice motion is shown to be influenced by the bottom topography at very low frequencies whilst tidal periodicities observed in the north-western Weddell Sea are below the level of the noise in the region of the study. In this area the higher frequency ice motion is mainly wind driven with little of the energy being transferred to the underlying deep water.

Received 22 August 1994, accepted 17 November 1994

Key words: Current meters, inertial oscillations, oceanography, sea-ice motion, tides, bottom water

Introduction

The formation of water masses and in particular Antarctic Bottom Water (AABW) has been relatively well studied; Foster & Carmack (1976), Whitworth & Nowlin (1987), Foster & Middleton (1980) and Foldvik *et al.* (1985) distinguished WSBW (Weddell Sea Bottom Water, θ<-0.7°C, where θ is the potential temperature) from the warmer AABW by a break in the θ–S curve. AABW is separated from water masses above by the θ = 0°C isotherm. Orsi *et al.* (1993) defined the bottom waters in the Weddell Sea entirely as WSBW and the overlying deep water separated from it by the -0.7°C isotherm as Weddell Sea Deep Water (WSDW). WSBW is derived by mixing of Circumpolar Deep Water (CDW) with shelf waters and this WSBW will mix upwards in time with overlying CDW which is warmer, more saline and poorer in oxygen, to replenish the overlying older WSDW.

The collection of long-term or short-term current meter data in the area south of the south Scotia Ridge and west of 25°W in the Weddell Sea has previously been very sparse (Fahrbach *et al.* 1991). We chose to study the north-west area (Fig. 1) as a site where newly formed WSBW is flowing away from its source and is close to intense mixing processes at the shelf break of the Antarctic continental shelf (Foster & Middleton 1980). Variability of the flow over very long time-scales can only be inferred from palaeoceanographic considerations, the longest periods of time that can be directly monitored are a matter of years. As part of a longer term study this paper presents and attempts to explain some of the oceanographic variability within this time span.

Previous research

In the Weddell Sea four major tidal constituents were found

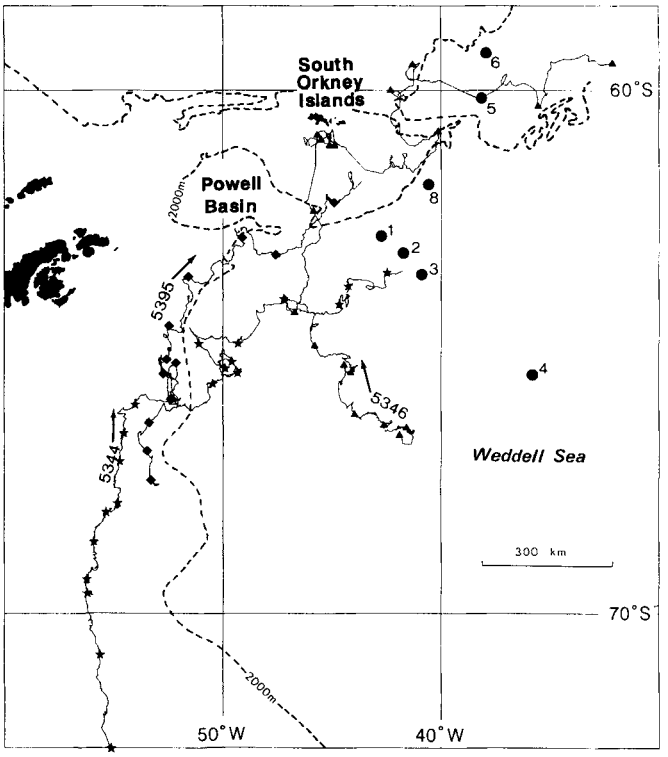

Fig. 1. Location of study area in relation to the Antarctic Peninsula. Mooring sites are numbered 1–8 (7 is missing). The tracks of buoys 5344, 5395 and 5346 and their direction of movement are shown in relation to the 2000 m contour. The symbols represent 10 day intervals for each of the three buoys. Start and end dates for tracks are; buoy 5344, 84/1989–307/1989, buoy 5346 (35/1990 – 236/1990) and buoy 5395 (346/1986–102/1987).

https://doi.org/10.1017/S0954102095000083 Published online by Cambridge University Press

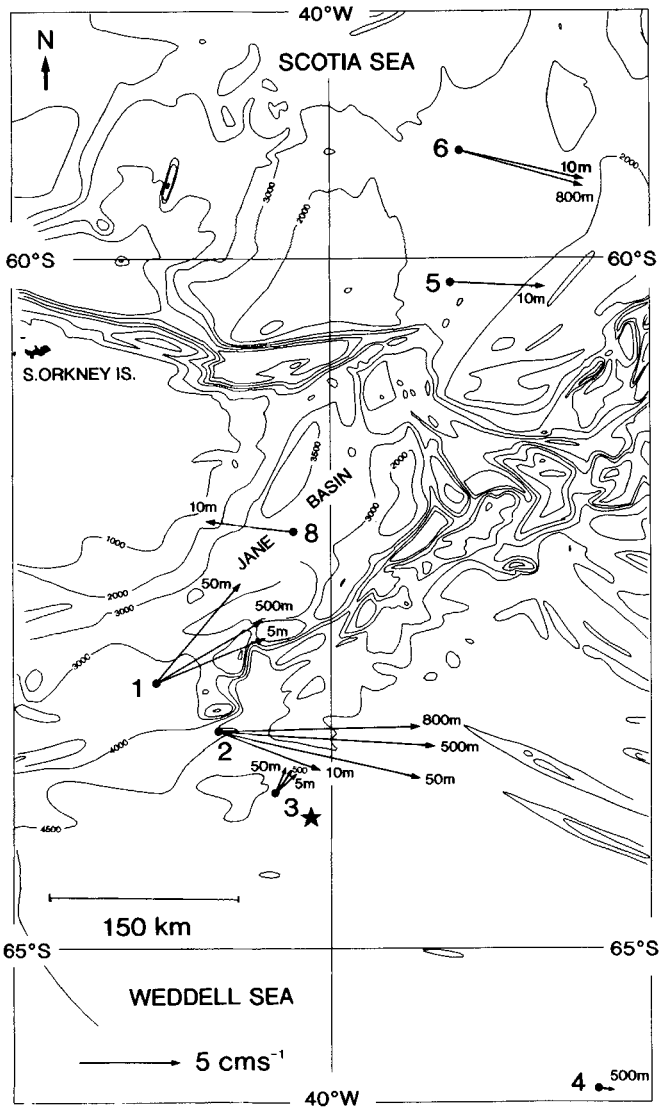

Fig. 2. Detail of bathymetry and mean annual velocity vectors at mooring sites. Length of arrow is proportional to the speed (scale shown) in the mean direction indicated. Height above the sea-bed is also indicated at the tip of the arrow. (*) marks position of CTD profile in Fig. 3.

(Irish & Snodgrass 1972) to propagate clockwise in the mixed diurnal and semi-diurnal regime. Foldvik & Kvinge (1974) noticed a large reduction in amplitude of the diurnal tides in mid-winter, which they thought could be due to homogenized shelf water being temporarily advected into the region of the current meters. In contrast, deep sea mooring data in the Weddell Sea (Middleton & Foster 1977) showed there was great similarity in energy between constituents and very little seasonal variation.

Our data give greater temporal coverage in an area farther north and west of any previously published results from the Weddell and Scotia seas. The area where these two meet is one of intense eddy activity and lateral shear (Patterson & Sievers 1980). WSBW is confined to the Weddell abyssal plain except near 25°W where it may extend north and fill the South Sandwich Trench. The Jane Basin does not provide a northerly escape route for the deepest bottom water, its exit sill depth being too shallow at *c.* 3000 m, and upstream gaps in the South Scotia Ridge are nowhere deeper than *c.* 1800 m (British Antarctic Survey 1985).

Rowe *et al.* (1989) examined periodic motions in the Weddell Sea pack ice. They concluded that the major periodicities were tidal, both diurnal and, to a lesser extent, semi-diurnal constituents, and that the power of the diurnal periodicity dropped by an order of magnitude in mid-winter due to internal ice resistance. Massom (1992) noted high coherence in the response of the ice motion over a large area, to the passage of storms.

Formation processes of WSBW

Our analysis of deep ocean current data in the north-west Weddell Sea has given us a better idea of the inherent variability and strength of bottom water flow. The forces which drive WSBW are complex and can only be understood when the processes of its formation are known in detail. Elements of the observed flow variability may be characteristic of bottom water formation processes and thus there is a need for the consistent deep ocean measurements that we show here.

The general cyclonic circulation and the Coriolis force tend to constrain the high salinity shelf water on the shelf, (Gill 1973). Foster & Carmack (1976) suggested that bottom topography may be an important factor in channelling the flow to the east and over the shelf edge.

In a hydrographic transect from the central Weddell Sea onto the north-western continental shelf in February 1976, Foster & Middleton (1980) interpreted a variation in bottom water properties downslope as evidence that the water had originated at different times or places, or both, along the shelf break and therefore had slightly different characteristics. The WSBW formed from this shelf water inevitably varies in salinity and density which gives rise to a dynamic eddy-like motion in the bottom layer (Foster & Middleton 1979).

Jenkins (1992) studied in detail sub-ice shelf processes that ultimately lead to bottom water formation and, together with Jenkins & Doake (1991), implied that bottom water formed from sub-ice-shelf processes will remain relatively constant and provide a large background volume, the observed short-term seasonal and inter-annual variability arising mainly from production of WSW in the west and mixing at the continental shelf break.

Foster & Carmack (1976) indicated that WSW may be formed all year round in varying quantities depending on the formation and movement of sea ice. The *total* sea-ice cover in the Weddell Sea sector of Antarctica undergoes enormous variation. In winter, at its maximum, it is about 7×10^6 km^2

https://doi.org/10.1017/S0954102095000083 Published online by Cambridge University Press

Table I. Mooring observations for all current meters.

Year and Rig No.	Position	Water depth (m)	Height above bed (m)	Number of days of data
87/88	63°10.7'S	3855	500	353
1	42°46.0'W		50	311
87/88/89	63°31.0'S	4580	500+800	351+410
2	41°45.9'W		50+50	351+412
87/88/89	63°56.6'S	4575	500+800	350+378
	40°54.0'W		50+50	350+411
			5	350+378
87/88	65°55.15'S	4770	500	270
4	35°49.4'W			
88/89	60°11.3'S	2969	10	288
5	38°8.6'W			
88/89	59°8.8'S	2870	800	159
6	37°57.6'W		10	373
90/91	62°4.5'S	3375	10	338
8	40°35.7'W			

which decreases to 1–2×10^6 km^2 in summer (Zwally *et al.* 1983). The *local* production of sea ice is dramatically affected by the prevailing winds and subsequent opening of leads and coastal, latent heat polynyas, so the accumulated local freezing may easily exceed the average freezing over the open ocean by an order of magnitude. Tidal stirring also helps in creating and maintaining open water areas, and on the continental shelf amplification of certain tidal components occurs (Foldvik *et al.* 1990) which enhances this effect.

Data collection

We look at data from seven current meter moorings from the area shown in Fig. 1 to examine the near-bottom circulation and also to compare and contrast properties of the surface motion in the region using drifting buoys deployed into sea ice floes.

Fig. 2 shows the location of the current meters in relation to the bathymetry (see also Table I). All meters were positioned within 800 m of the sea bed. The typical temperature-salinity profile in Fig. 3, from this region of the Weddell Sea (marked in Fig. 2), shows the vertical extent of WSBW. Useful data were obtained from a total of 13 Aanderaa model 5 and 8 meters (Table I).

Moorings 1,2,3 & 4 were deployed in late austral summer of 1987 and recovered a year later when meters 1,2 and 3 were re-deployed. In March 1989 three moorings were laid farther north (5,6 & 7) to look at the region of the Weddell-Scotia confluence and the coupling of Weddell Sea water with water flowing east from Drake Passage. Figs. 1–7 were then retrieved in 1990. Rig 7 had failed completely, 1 & 3 were redeployed and a further mooring, Rig 8, was laid in Jane Basin to look at bottom water flowing north through this gap in the South Scotia Ridge. The current meter data comprise speed, collected as an average value over a sampling interval of one hour, and a corresponding direction recorded as an instantaneous reading. In addition, some of the lowest meters housed a thermistor for temperature measurement in the range -2.64 –5.62°C.

Drifters consisted of a vertical assembly of instruments comprising a current meter suspended 10 m below an ice mounted buoy on top of which was mounted an anemometer. Internal instruments were fluxgate compass, barometric pressure gauge and ARGOS transmitter, surmounted by an antenna and air temperature sensor. Drifter 5395 deployed in January 1986 in the south-west Weddell Sea, drifted northwards along the western side of the Weddell Sea and, during the first four months of 1987, moved into the area of the moorings. Ice beacon 5344, air-dropped at the beginning of 1989, moved with the general clockwise circulation and was in the north-west Weddell Sea in September–November of the same year. Buoy 5346 was deployed in early 1989, and was moving through the area of the moorings in April, May and June 1990.

The drifter positions and sensor data were transmitted at irregular intervals up to 3 h apart, dependent upon the satellite orbital parameters. Consecutive positions were used to calculate ice drift velocity vectors. Sensor data for each satellite pass were median filtered and then all data were interpolated to hourly intervals.

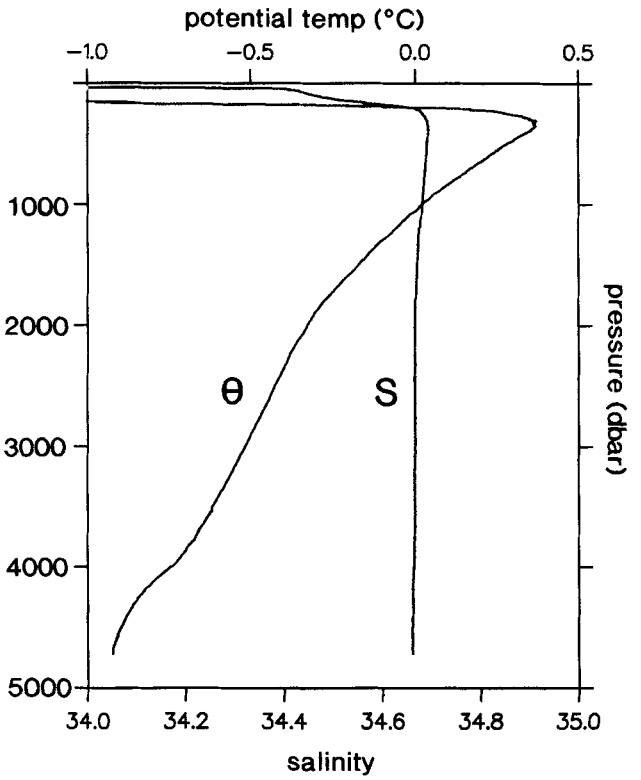

Fig. 3. Deep ocean potential temperature and salinity profile for Weddell Sea at position marked in Fig. 2 by (*). The cast was taken on the 1988 cruise.

https://doi.org/10.1017/S0954102095000083 Published online by Cambridge University Press

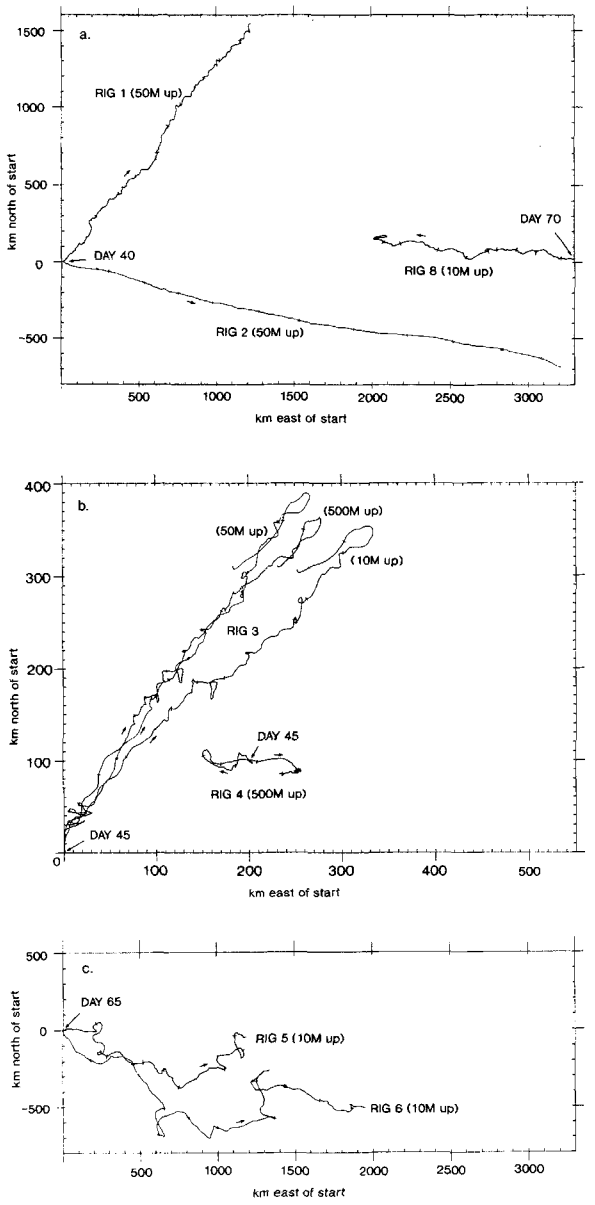

Fig. 4. Progressive vector diagrams from de-tided data at **a.** Rigs 1, 2 (1987/88) and Rig 8 (1990/91), **b.** Rigs 3 and 4 (1987/88), **c.** Rigs 5 and 6 (1989/90). Crosses mark 30 day intervals.

Data analysis

Current meter data

In the Weddell Sea some of the main features of note (Fig. 4) are the flow to the NE channelled strongly out through Jane Basin to the Scotia Sea, observed at Rig 1, and the stronger flow to the ESE at Rig 2 to the south. Marked scouring seen on sub-bottom acoustic profiler records (Pudsey *et al.* 1988) suggests that the water flowing past Rig 2 was constrained spatially both by the topography of the South Scotia Ridge and the Coriolis effect as a boundary current.

At Rig 3 the flow was variable on time scales of 5–10 days, and the passage of mesoscale current fluctuations was observed throughout the year, occurring simultaneously at all levels up to 500 m above the sea floor. The current reversal observed at Rig 3 could be attributed to a slow-moving eddy although there is no appreciable change in the corresponding temperature record and it is not clear in which sense the eddy would be rotating. Such mesoscale eddies have also been observed in the western Weddell Sea by Foster & Middleton (1979) and attributed to baroclinic instabilities.

Flow at Rig 4 was the least energetic and the record shows that the rotor was stalled almost 50% of the time. The ambient current was at or below the stalling speed of 1.1 cms^{-1} for almost half the year. There is a very small net south-easterly component but overall flow was dominated by tidal oscillations. Mean flow at Rig 8 indicates some recirculation at least within the deepest part of Jane basin.

Flow in the southern Scotia Sea was very energetic with greater long term variability in direction than in the Weddell Sea and current variations on time scales of between 10 and 30 days (particularly at 10 m above the sea bed). Seasonal trends in N-S velocity are evident at both Rigs 5 and 6, 125 km apart. These two Rigs lay within the Weddell Scotia Confluence (Foster & Middleton 1984) where deep mixing occurs (Deacon & Moorey 1975, Deacon & Foster 1976) in *c.* 3000 m water depth.

Table II shows that the kinetic energy (KE) densities from unfiltered data increase from south to north, with the lowest values being towards the centre of the gyre. In general the KE density, 10 or 50 m up from the bed, tends to be higher than at 500 m up. This reflects a higher-energy environment due to mesoscale fluctuations and low frequency variability such as topographically induced eddies and turbulence.

Surface current characteristics

The trajectories of the three ice-mounted drifters (Fig. 1) show a clear northwards trend in the Weddell Sea as far as the South Scotia Ridge, where topography and the influence of westerly winds causes an eastward motion. Buoys 5395 and 5344 drifted to 64°S and 66°S respectively before turning east following the line of the shelf on the southern side of Powell Basin. In April 1990 buoy 5346, some 5–10 degrees farther to the east, reached 61°S before turning east close to the South Orkney Islands. These differences are consistent with the longitudes at which the buoys were moving and with some effect on the surface circulation by the bottom topography.

Fig. 5 shows an example of the velocity vector components for drifter 5346 for the period when it was in the area of the current meters. Two things are clear; the magnitude of the ice motion is much larger than that of the bottom currents previously described, and large irregular variations occur with periods of a few days. Although small perturbations in the velocity components are visible with periods of *c.* 12 h, most of the ice motion is due to wind forcing, with the period of variations (4–5 days) corresponding to the passage of low

https://doi.org/10.1017/S0954102095000083 Published online by Cambridge University Press

Table II. Basic current statistics.

Rig No. and height above bed (m)	Mean values over total velocity record E (cms^{-1})	N (cms^{-1})	Speed (cms^{-1})	*In-situ* Temp. (°C)	Direction and magnitude (mean velocity vector) (cms^{-1})		Kinetic energy density
1 (500)	5.497	3.232	9.245	-0.518	59.5°	6.38	32.71
1 (50)	4.384	5.331	9.703	-0.662	39.4°	6.90	36.94
2 (500)	11.268	-0.523	11.735	-0.446	92.7°	11.28	20.23
2 (50)	10.584	-2.264	11.445	-0.516	102.1°	10.82	19.60
3 (500)	0.765	1.026	2.638	-0.492	36.7°	1.28	4.53
3 (50)	0.602	1.026	3.188	-0.633	30.4°	1.19	6.51
3 (5)	0.831	1.011	2.757	-	39.4°	1.31	4.97
4 (500)	0.152	-0.066	1.550	-0.504	113.3°	0.17	0.96
5 (10)	4.763	-0.222	10.514	-	92.7°	4.77	77.64
6 (800)	6.31	-1.69	9.680	0.038	105.0°	6.53	35.43
6 (10)	6.039	-1.589	12.434	-0.425	104.7°	6.24	61.77
8 (10)	-4.38	0.501	6.840	-0.663	276.6°	4.41	22.17

Direction is measured clockwise from north and kinetic energy density in $[(cm/s)^2 cph^{-1}]$.

pressure systems. A comparison of wind speed and the speed of the ice relative to the water, from an area just south of the study area (before the failure of the current meter on the buoy) reveals a correlation coefficient of 0.7 and current to wind speed ratio of 1.5%, indicating that wind is the predominant forcing mechanism in this region.

Hibler & Ackley (1983) found ice velocity characteristics in the Weddell Sea to be largely wind-driven with the exception of the area near the Peninsula where the internal ice stress becomes important, causing the ice to turn northward with greater velocity.

Analysis of the tracks of all three drifters shows that in the western Weddell Sea, the dominant tidal components of ice motion are diurnal. Farther north, in the area of this study, the tidal components in the surface circulation are below the level of noise, the frequency of inertial motion showing the most significant peak. The variations in power of the inertial component and higher frequency ice motion are greater in periods of low ice concentration (values obtained from passive microwave data) and this, along with similar changes in inertial power at some of the current meter sites, reinforces the possibility that seasonal variations in the ice cover may be affecting the currents throughout the entire water column.

Annual variability in mean currents

The amplitudes of current velocities and the corresponding temperatures varied seasonally (see Fig. 6a & b). Mean velocity and temperature values (from the current meter thermistors) over 30-day periods throughout each record were compared, resolving the velocity in the direction of the record mean (normally taken over about 360 days). To obtain significant estimates of inter-annual or even seasonal variability, several years of data are required. We have two consecutive years at most, and can therefore obtain only a qualitative assessment of periodicities and magnitudes of change from these data. Unfortunately there are no thermistor data from any of the meters 5 or 10 m above the sea bed. All velocity and temperature plots show annual fluctuations, with warmer temperature values corresponding to higher current velocities. This contrasts with the observations of Foster & Middleton (1979), to the south of Rig 2, which showed colder events associated with higher current velocities, especially during the summer.

The vertical coherence of current velocity is strong, and periodicities of a combination of annual and semi-annual variations are observed. Low frequency oscillations of about 5 or 6 days, caused by low pressure systems, were found to have a deep reaching effect in weakly stratified regions such as this (Baker *et al.* 1977). Sarukhanyan (1986) attributed such fluctuations to changes in the intensity of the zonal geostrophic wind over the Southern Ocean, or to the semi-annual solar tidal waves in the ocean. According to

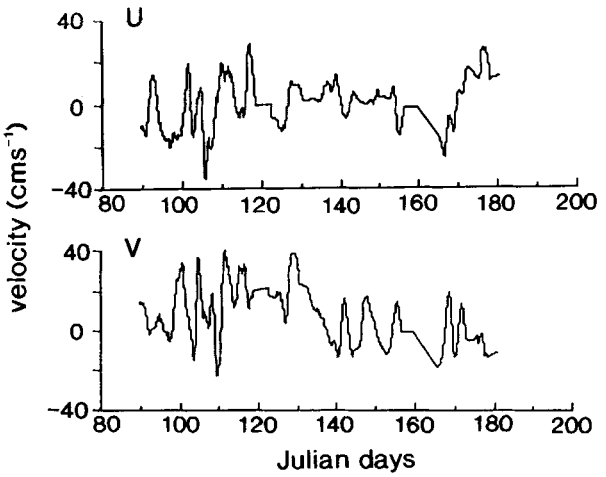

Fig. 5. U and V velocity components of drifter 5346, relative to the ground in Julian days from the start of 1990.

https://doi.org/10.1017/S0954102095000083 Published online by Cambridge University Press

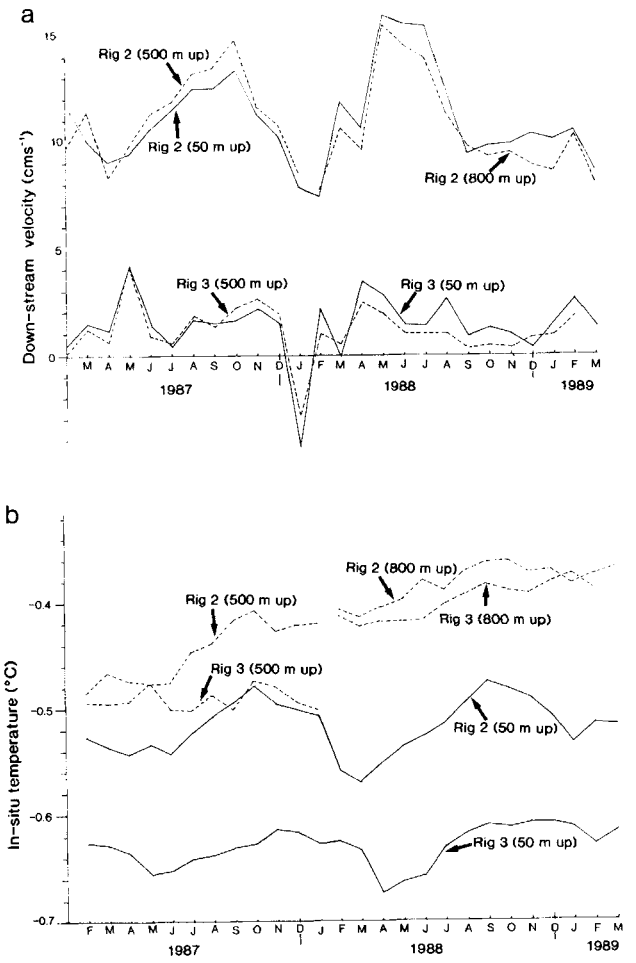

Fig. 6. a. Down flow components of mean monthly velocity and **b.** mean monthly temperature values at Rigs 2 and 3 as annotated, for two consecutive years of data.

Sarukhanyan (1986), the maximum of the solar semi-annual tide at high latitudes occurs at the end of June and December. At Rig 3 maxima occurred in May and November so there was a phase lead of one month if this was the cause. At Rig 2, where the strongest mean flow was recorded, the seasonal variation was dominant.

Bottom water is supplied from the continental shelves to the abyssal plain as a thermohaline flow which varies seasonally (Foster & Middleton 1979). They suggested that this variability was due to increased rate of formation of bottom water during winter, with observed year to year differences due to variations in sea ice formation. The temperature of the relatively thin layer of cold bottom water (Fig. 3), monitored at other rigs, also fluctuates seasonally, but corresponding changes in current strength do not always occur.

The annual mean *in-situ* temperature in Weddell Sea records is everywhere less than -0.4°C, (except at Rig 6, 800 m up) which corresponds to -0.7°C potential temperature or the upper limit for WSBW. The temperature records fluctuate about the mean and the degree of this variation (measured as standard deviation) is greatest (for the current meters in the Weddell Sea) at Rig 1 500 m up. The values are even larger in the Scotia Sea. At Rig 8 the mean temperature (the only record from a basal meter) was the lowest of all sites. The mean flow there indicates that this bottom water was not escaping north but recirculating within the basin. However, a near-bottom, westward-flowing counter current of cold AABW exists in the Scotia Sea and Drake Passage (Nowlin & Zenk 1988); that water, originating from the Weddell Sea, has probably escaped out of Jane Basin. The sill depth of *c.* 3000 m prevents the deepest water at 3280 m escaping but still allows some of the very cold bottom water to move north at depths shallower than this if the bottom layer is at least 500 m thick. The height of the -0.7°C isotherm above the sea bed was between 500 and 600 m at each of Rigs 1, 2 and 3 when measured in February/March 1989. Once over the sill, the water can descend and flow west, trapped in a deep channel on the northern margin of the South Orkney microcontinent (Fig. 2).

Analysis of tides

Some of the small scale variability is obvious from the raw velocity and temperature data (Figs 7 & 8). Tidal oscillations occurred at all sites, and almost entirely dominated flow at Rig 4. At Rig 2 tidal oscillations were evident and lower frequency variability was also present at Rigs 1 and 2 over 7–15 day periods in higher energy bursts above the mean. Rig 6 was the highest energy site and records show high frequency variability superimposed on high energy, eddy-like fluctuations making the time series far less uniform in appearance. The maximum variability observed from records in the Weddell Sea is always in the direction of mean flow but the Scotia Sea records show much greater cross-flow variation.

To investigate frequencies present in the time series, a harmonic analysis was performed on the whole length of the available data sets (using software made available by the Institute of Oceanographic Sciences) and tidal ellipses were generated for each of the major components (M_2, S_2, K_1 and O_1). The ellipticity and size of the major and minor axes reflect the energy in each component, and effects of topography and bottom friction on the tidal wave. The ellipse can also be represented as the sum of clockwise and counterclockwise circles whose proportions vary according to the tidal composition. Table III gives the ellipse parameters from each meter at Rigs 1–6. The sense of rotation for almost all constituents calculated over the entire period of data at the Weddell Sea sites was clockwise. At Rigs 5 and 6, the S_2 constituent showed anticlockwise rotation at the lowest meter and at Rig 6 there was anticlockwise rotation in O_1. The tidal wave in the Weddell Sea acts as a Kelvin wave and is trapped against the coastline, forcing the clockwise rotation. The Kelvin wave has a wave speed c_0 equal to $(gh)^{1/2}$. For the main semi-diurnal tide in an ocean of depth 4400 m it produces a

https://doi.org/10.1017/S0954102095000083 Published online by Cambridge University Press

wavelength of 9000 km which decays exponentially away from the coast, so that tidal velocities at the gyre centre would be expected to be the smallest. The main Southern Ocean tide propagates westward around Antarctica (Foldvik *et al.* 1990). Huthnance (1983) modelled the diurnal tide as a Kelvin wave circuiting an idealized (circular) Antarctica with a natural period of about 30 h. He observed that O_1 was enhanced relative to K_1, its natural period being closer to the proposed Kelvin wave. A marginal enhancement of O_1 over K_1 of *c.* 10% is observed in ellipse data from Rig 6 at 800 m up (the bottom meters are subject to friction and therefore discounted). He compared output with Scwiderski's (1981) interpolation of global ocean tides. However, observations of tides in the Weddell Sea are very sparse, and model comparisons need more data coverage to be useful.

The current meter record from Rig 8 indicates larger tidal amplitudes than from any of Rigs 1–4, although the magnitudes from all rigs reflect what would be expected from relatively small, deep sea tides. The increased magnitude may be due to the confinement and amplification of the tidal wave at depth as it rotates clockwise as a form of Kelvin wave. The local topography there may also cause some enhancement. Sarukhanyan (1986) noted that an increase in tidal current velocities can occur in near bottom layers especially in canyons associated with the generation of resonance oscillations of the tidal wave. At great depths, an increase may also be associated with the vertical density distribution and the baroclinicity of tidal currents. Comparison of tidal magnitudes with those obtained for similar record length and position by Middleton & Foster (1977) in the central Weddell Sea show very similar results in all respects.

Rig 2 data were divided into successive quarters for tidal analysis. We found much more variation in size and orientation of component ellipses at Rig 2 than was observed by Middleton & Foster at their site (closer to Rig 3) in all quarters, particularly from November–January 1988. This coincides with the increased variability observed in the mean flow over the austral summer also observed by Foster & Middleton (1979).

Spectral analysis

The hourly time series of current velocity and temperature were also used to evaluate clockwise and anticlockwise rotary spectra. Tidal frequencies gave significant energy peaks as did the inertial motions discussed later. Diurnal and semi-diurnal tidal peaks appeared in spectra from every position, but generally in the more energetic areas of flow these peaks are less prominent, especially in the Scotia Sea at Rigs 5 and 6 where there was more noise at all frequencies. The overall tidal energy gradually decreased from north to south in all rigs, consistent with the Kelvin wave decaying towards the centre of the Weddell Sea. Semi-diurnal components dominate over diurnal in the north but this is gradually reversed toward the south.

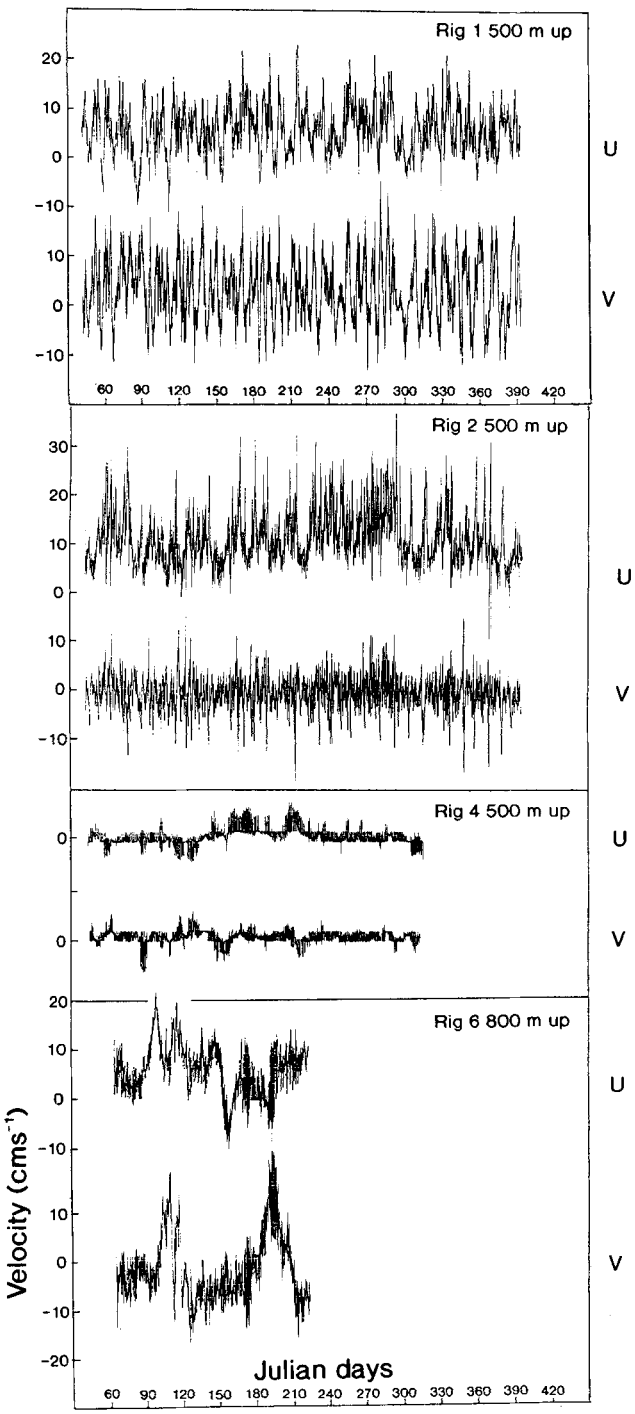

Fig. 7. Unfiltered velocity, resolved into its constituent components for each of the Rigs 1,2,4 and 6.

In all spectra there is a rise in energy continuum around the diurnal and semi-diurnal frequency bands. These represent tidal cusps due to the baroclinic components of the flow not being phase-locked to the tide-producing forces, as are the barotropic tidal components.

https://doi.org/10.1017/S0954102095000083 Published online by Cambridge University Press

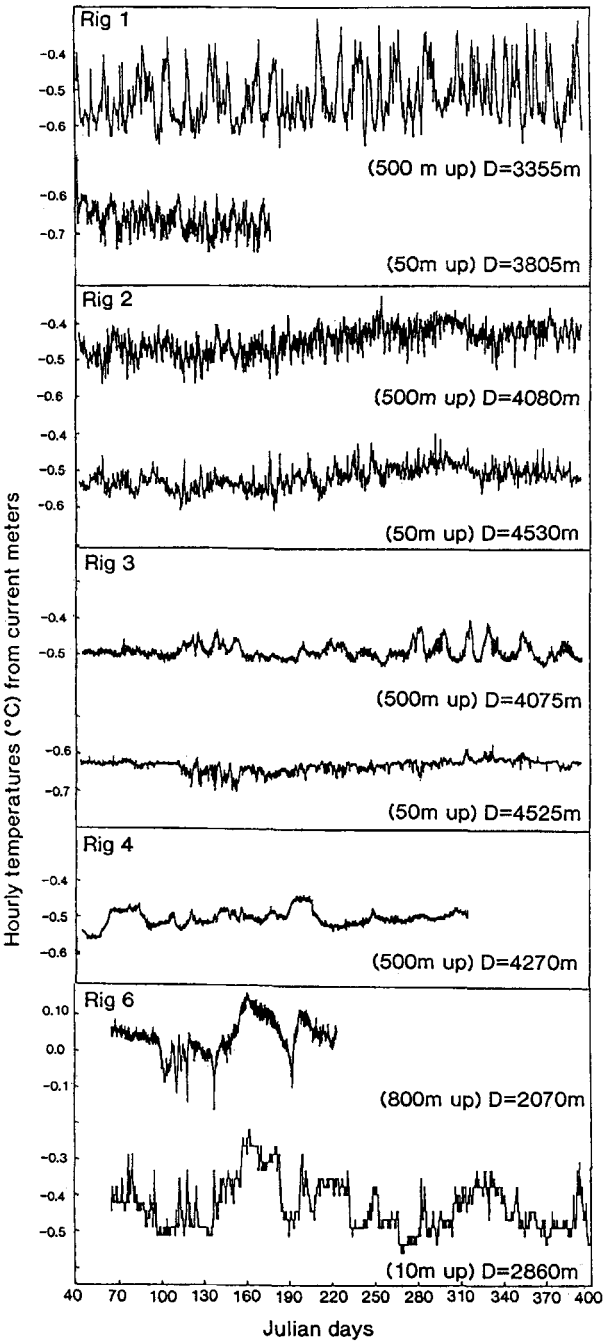

Fig. 8. Unfiltered temperature records for Rigs 1,2,3,4 and 6.

Inertial oscillations

Peaks of energy at inertial frequencies were found at all sites except Rig 2, indicating that there is likely to be a common causal mechanism. Motion at the inertial frequency is generated when some force (e.g. wind) acts in the same direction for a period of time, causing the water to accelerate, and then stops, when the water continues to move as a consequence of its momentum. The moving mass of water is acted on by the Coriolis force, giving rise to a circular trajectory and thus to a periodic motion. The frequency of the motion is latitude-dependent and the amplitude varies depending on the strength of the generating force. The oscillations decay due to friction after the generating force stops. Middleton & Foster (1977) found inertial peaks to be indistinguishable from the noise in similar data from the Weddell Sea. The inertial frequencies at the mooring sites ranged from 0.07628 counts per hour (cph) at Rig 4 (farthest south) to 0.07174 cph at Rig 6 (farthest north). These are close to the semi-diurnal tidal frequencies (M_2, 0.08051 cph and S_2 0.08333 cph), but are separable from the tidal peaks by examination of the rotary spectra at this latitude.

Webster (1968) reviewed observations of inertial oscillations from deep-sea locations at all latitudes, finding that the vertical extent was thin, of the order of several hundred metres, and that the oscillations had an intrinsically transient nature with endurance times of only a few days. This makes their identification difficult as the length of data necessary to resolve inertial motions may be longer than the lifetime of the motions. The mechanisms of generation are varied. Near the surface, variable wind stress associated with the passage of weather systems will induce near-surface oscillations, often reaching maximum values at density discontinuities (i.e. at the pycnocline) but thereafter decreasing with depth. Alternatively any impulsive change in flow by thermohaline effects or flow over topography could cause bottom-generated inertia currents which may then propagate upwards. In Drake Passage, large storms and deep-reaching weather systems have been shown to induce inertial oscillations at depths greater than 3500 m. Rig 6 may have registered some of the effect of these deep-reaching forcing factors even though it was located considerably southward of the axis of the ACC. A potential source of energy for creation of inertial oscillations comes from the Weddell-Scotia Confluence (Patterson & Sievers 1980, Foster & Middleton 1984) with its strong lateral shear and consequent instabilities. Data from Rig 6 show a high and broad inertial peak at 800 m up in this region.

To investigate the variation in inertial power over a period of time, clockwise and anticlockwise spectra were generated for all the meters at Rig 3, using overlapping 88 day segments through the year. The inertial component was calculated as the difference between the anticlockwise and clockwise power at the inertial frequency. Fig. 9 illustrates the seasonal variation in inertial energy. There is a large variation at all depths, with greater than an order of magnitude reduction during the winter period. In contrast, the barotropic semi-diurnal tidal oscillations maintain a more constant level throughout the year (Fig. 10). It is tempting to attribute this reduction to the seasonal increase in the sea ice extent. McPhee (1978) demonstrated that the formation of a consolidated sea ice cover helped to prevent momentum transfer to the underlying ocean, thus reducing inertial motion in the surface layer and hence inducing an abrupt change in amplitude from summer to winter. A comparison with typical ice extent variation in the Weddell Sea sector

https://doi.org/10.1017/S0954102095000083 Published online by Cambridge University Press

Table III. Tidal current ellipse data.

Rig No.		Major axis	Minor axis	Incl.[1]	Phase		Major axis	Minor axis	Incl.[1]	Phase
1 (500)	M_2	0.858	-0.515	60.7	-93.4	O_1	0.322	-0.005	-72.1	83.9
	S_2	0.769	-0.239	83.6	-73.3	K_1	0.800	-0.163	-47.0	131.7
1 (50)	M_2	0.956	-0.282	-90.6	69.5	O_1	0.267	0.044	-41.5	98.1
	S_2	0.884	-0.119	89.2	-70.1	K_1	0.735	-0.292	-35.6	131.8
2 (500)	M_2	0.851	-0.547	-16.0	43.6	O_1	0.580	-0.252	-1.9	154.5
	S_2	0.756	-0.323	119.8	-43.3	K_1	0.963	-0.363	10.9	144.3
2 (50)	M_2	0.705	-0.585	-23.6	24.9	O_1	0.463	-0.339	89.6	35.9
	S_2	0.797	-0.202	-68.0	111.0	K_1	0.712	-0.448	-18.2	153.4
3 (500)	M_2	1.007	-0.088	37.8	-48.2	O_1	0.651	-0.387	5.5	-61.6
	S_2	0.543	-0.245	40.1	27.2	K_1	0.716	-0.419	21.7	-29.6
3 (50)	M_2	0.849	-0.308	30.2	-61.1	O_1	0.671	-0.434	-1.6	135.1
	S_2	0.634	-0.200	44.0	-38.4	K_1	0.756	-0.483	9.5	128.5
3 (5)	M_2	0.397	-0.173	30.3	82.5	O_1	0.358	-0.297	-16.7	-138.1
	S_2	0.365	-0.119	45.8	105.9	K_1	0.331	-0.317	-162.6	16.3
4 (500)	M_2	0.578	-0.148	44.6	-91.0	O_1	0.586	-0.358	-2.6	-161.4
	S_2	0.280	-0.137	50.1	-113.4	K_1	0.507	-0.275	-0.2	77.8
5 (10)	M_2	1.275	-0.280	44.6	-11.3	O_1	1.143	-0.324	-68.1	-84.1
	S_2	1.363	-0.402	50.1	-24.5	K_1	1.230	-0.581	-81.7	-67.3
6 (800)	M_2	1.102	0.114	37.7	-9.2	O_1	1.010	0.200	-62.6	-106.8
	S_2	0.729	0.170	89.3	11.9	K_1	0.981	-0.109	-63.3	-94.2
6 (10)	M_2	1.304	-0.036	44.7	-36.0	O_1	1.011	0.274	105.1	66.9
	S_2	0.795	0.062	78.9	-7.7	K_1	0.704	-0.096	-71.6	-84.8
8 (10)	M_2	1.134	-0.258	61.9	-6.0	O_1	1.011	-1.306	77.8	92.1
	S_2	1.102	0.069	90.2	-97.0	K_1	0.704	-1.028	-100.2	-69.7

[1]Included is the angle east from north of major axis direction. Axis units are cms^{-1}.

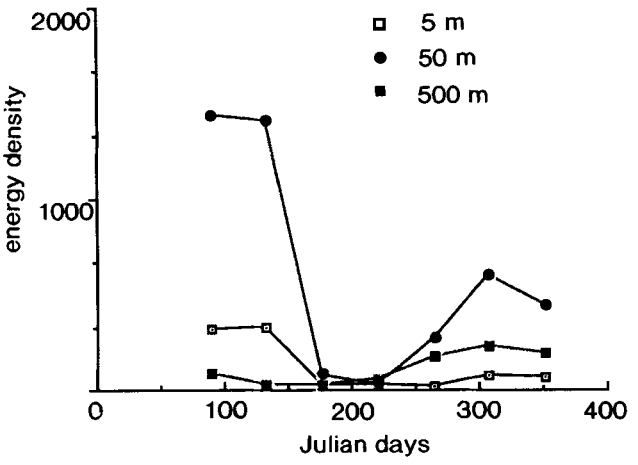

Fig. 9. Mean seasonal spectral energy density at the inertial frequency for Rig 3 at 5,50 and 500m above the sea-bed.

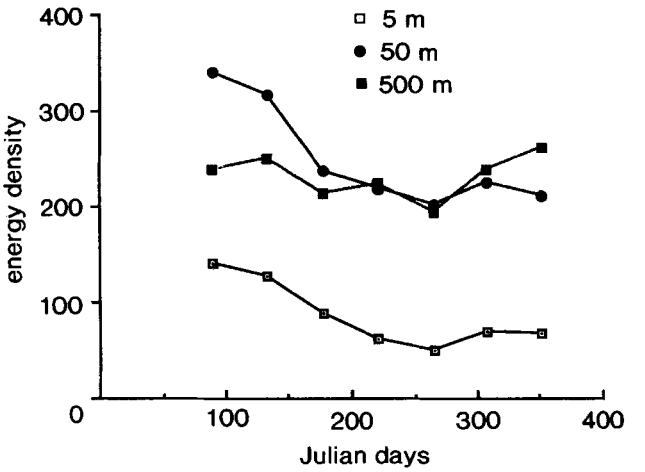

Fig. 10. Mean seasonal spectral energy density for the M_2 tidal component at Rig 3, 5, 50 and 500m above the sea-bed.

(Zwally *et al.* 1983), however, shows that the reduction in inertial power at the mooring sites coincides not with maximum sea ice extent but with the maximum rate of growth.

To examine this relationship, power at the inertial frequency is plotted in Fig. 11 as a time series for both a surface drifter and current meters. There is no obvious connection between the presence of inertia currents at the surface and the bottom. The current meter data from 50 m up at Rigs 1 and 3 show substantially greater energy at the inertial frequency than from higher in the water column. This indicates a bottom-generating mechanism which could be related to variations in the production and flow of WSBW from the continental margins to the west. Currents near the sea bed are attenuated by bottom friction, which is evident in the lower power present at all frequencies at the bottom meter. At Rig 2 there was no inertial energy because of its proximity to the basin

https://doi.org/10.1017/S0954102095000083 Published online by Cambridge University Press

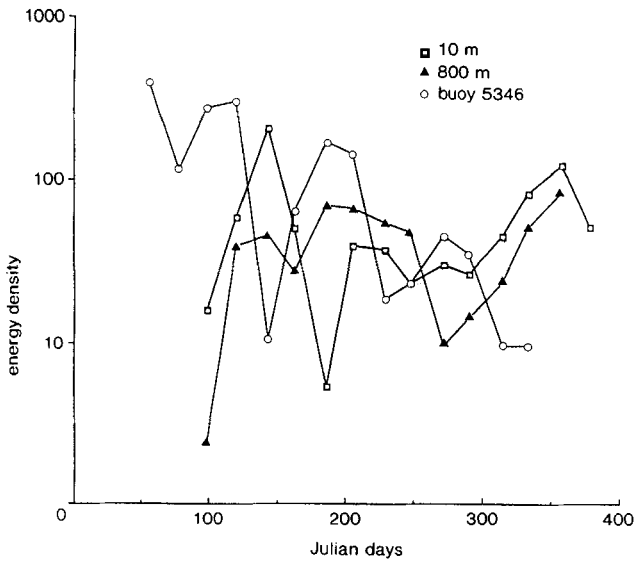

Fig. 11. Spectral energy density at the inertial frequency at Rig 1 at 10 m and 800 m above the sea-bed compared with that from drifter 5346 at the surface.

margin inhibiting the anticlockwise motion.

Higher power at the inertial frequency from Rig 3 data coincides with greater variability and magnitudes in the mean velocity values (and with lower temperature values, see Fig. 8), a feature most prominent at the middle meter. Foster & Middleton (1979) obtained similar results from a single current meter in the central Weddell Sea. They attributed this increased variability to the intermittent nature of the formation and flow of bottom water. As the maximum rate of ice growth, and thus salt rejection, occurred around day 160 in the Weddell Sea sector, and the increase in the variability of the bottom water was not until approximately day 250, this implies a time delay of around 3 months before the pulse of new bottom water reached the north-west Weddell Sea.

Inertial motions are damped by friction and the vertical height of frictional influence of flow over topography is governed by Ekman's equations. The currents at two levels within the Ekman layer can be used to solve for the unknown Ekman depth, D_E, and hence eddy viscosity. Using mean yearly values obtained for Rig 3, at 5 and 10 m above the sea bed, and resolving in the direction of free stream velocity at 800 m, we estimate the Ekman layer to extend approximately 21 m above the bed. The value for eddy viscosity, A_z, from $D_E = \pi(2A_z/f)^{1/2}$ where f is the Coriolis parameter, is 0.003 m^2s^{-1}. Therefore the depth of frictional influence appears to be contained entirely within the layer of WSBW (Fig. 3).

Coherence estimates

Estimates of rotary coherence for the clockwise and anticlockwise rotary components of velocity were made using equivalent sections of the time series from different meters on the same and different rigs, and ARGOS buoy 5395.

At each rig in the Weddell Sea there is coherence at the 99 % confidence level for all the major tidal frequencies in the clockwise component between all meters. Only values of coherence at the 99% level and above are considered. Coherence between the closest meter pairs i.e. between the meters at 10 m and 50 m above the bottom, is greatest. There is no coherence between meters at frequencies higher than the semi-diurnal tides nor in the anticlockwise component at inertial frequencies at Rig 2. Coherence is high at semi-diurnal tidal frequencies which arise from the presence of tidal cusps, the interaction of semi-diurnal and inertial components. At frequencies lower than tidal, specifically with periods of 7–14 days, 21 days and 42 days, there is high coherence in clockwise and anticlockwise motions between all levels of the same rigs. Foster & Middleton (1979) in a comparable study, found the periods of allowable modes of standing waves at 66°30'S for an ocean depth of 4500 m to be $T_0 = 10$ days, $T_1 = 23$ days and $T_3 = 43$ days. The barotropic part of the tidal wave is vertically coherent on the same rig for these periods and correspondingly the oscillations were virtually in phase, gradually moving out of phase and less coherent at periods less than about three or four days.

Coherence between meters at the same vertical height from the seabed but adjacent rig positions was only evident at the major tidal components in the clockwise sense in the Weddell Sea. In the Scotia Sea, the data were limited but high coherence was seen at meters 10 m off the bed between Rigs 5 and 6 in the anticlockwise component and diurnal tidal frequency. In the Scotia Sea the tidal wave propagates westwards and hence should show up in the anticlockwise expression. Data from the window of time when the ARGOS buoy 5395 was in the same area as Rig 1 were used to make an estimate of coherence through the water column from the surface to the meter at 500 m above the seabed. The coherence was very poor and only reached the 99% confidence level for the anticlockwise component at a frequency close to the diurnal tide.

We conclude that vertical coherence over relatively small spatial scales (up to 800 m) is much higher than the lateral coherence over scales of 40–60 km (distances between rigs). The lateral extent of even the low frequency oscillations is less than 60 km. The only periodicities that are due to widespread non-localized phenomena appear to be of tidal origin. Bryden (1979) and Pillsbury *et al.* (1979) also found that high coherence of currents in the upper 1000 m was maintained in the deepest layers in the Drake Passage, though the horizontal correlation of the currents was weak.

Discussion

Antarctic pack ice is seen as a sensitive indicator of climate variability (Zwally *et al.* 1983) and its concentration and extent have been linked with the pressure/wind system of the Southern Oscillation (Carleton 1988). This implies that the

https://doi.org/10.1017/S0954102095000083 Published online by Cambridge University Press

cyclicity of formation of bottom water may also be linked to ENSO (El Ñino Southern Oscillation) events and some of the long-term variability of the pressure/wind system.

The annual cycle of sea-ice extent and the interaction between sea-ice anomalies and atmospheric circulation, analysed by Lemke *et al.* (1980), showed there to be a marked asymmetry in the growth-melt cycle (fast melting, slow freezing) in data from 1973–79. This was also demonstrated by Zwally *et al.* (1983) in an analysis of Antarctic sea-ice extent. Gordon (1981) attributed the seasonality of the sea-ice to Ekman divergence, which influences the sea-air exchange. In spring it induces upwelling of warm deep water, enabling greater melting and, in winter, enhances the formation of sea-ice in the interior of the ice fields rather than accretion at the outer edge. Such an asymmetry appears in the mean monthly temperature records over two consecutive years at Rigs 2 and 3 (Fig. 9). The fact that the peaks and troughs of our data and sea-ice extent data roughly coincide is misleading, because there will inevitably be a time lag between formation of the WSW and its appearance at our rigs incorporated into WSBW. However, the lag may be a multiple of a year. Foster & Middleton (1980) suggested that bottom water may have taken at least a year to travel from the shelf break to their mooring site in the Weddell Sea, undergoing considerable modification by mixing with water from above. The mean current velocities, particularly at Rig 3, do not show this asymmetry, which may indicate that the properties of bottom water (e.g. the temperature) are directly affected by seasonal sea-ice changes but the supply to the abyssal plain is not.

Our observations and those of others show that periodic sea-ice motion is governed primarily by meteorological phenomena. The passage of low pressure systems is evidenced by 4–5 day periodicities in the ice velocity vectors. Atmospheric disturbances provide impulses resulting in inertial motion with greater energy density than the tides. Energy exchange directly from surface to deep ocean is inhibited by ice cover in the whole Weddell Sea during winter and in the south and west all year round, but in the Scotia Sea, where ice cover is much less over most of the year, more energy transfer occurs. Large peaks in energy at the inertial period are very prominent in the data from the Scotia Sea moorings.

In deep water, inertial oscillations can only occur if the flow is unconstrained. In the Weddell Sea, inertial oscillations probably arise from impulsive changes in thermohaline flow over bottom topography. Internal waves may travel along the horizontal interface between water masses and also cause turbulence and inertia currents in the deep water. Temperature records show considerable variability, particularly in data further above the sea-bed, and a 10–15 day oscillation is evident in most. Those meters in the Weddell Sea at 500 m above the sea bed were close to the interface between WSBW and AABW. Although this is not a very sharp boundary there is a change in the slope of the θ-S profiles.

There were large seasonal variations in the power of the inertial component in the deep ocean and these were most likely to be due to differences in the variability and magnitude of WSBW flow but not necessarily production. During winter the power of inertial oscillations was small. In summer, however, the power of inertial oscillations increased more than tenfold, rising to more than three times the power of the strongest tidal components; this was most evident at 50 m from the sea bed.

The seasonal signal of current flow may be an artefact of the transport rather than actual production. For example, if the wind-driven circulation increases during winter, then, by continuity, the inflow of bottom water off the shelf may also increase provided its salinity is high enough to allow it to flow down the slope under the WDW. Thus WSBW is effectively being pulled down slope by a change in strength of the Weddell Gyre.

Seasonal variation in shelf-break mixing, induced by shelf waves and tides (Foster *et al.* 1987), may be responsible for a production signal. The situation is complex and it may well be that one process dominates over another at different times of the year and the bottom water passing our moorings does not always come from the same source all the time.

The tidal wave is a cyclonic Kelvin wave in the Weddell Sea with maximum tidal velocities at its margins, and an anticyclonic wave circum-navigating the continent north of the south Scotia Ridge. Harmonic analysis shows that the components are everywhere mixed with some variation in the relative sizes, which fits with tidal models in the Southern Ocean. The overall energy density observed from deep sea currents is greatest in the northernmost moorings. Most energy is found at low frequencies everywhere; the seasonal variation has a semi-annual and annual cycle arising from differences in production of bottom water and flow from its source which may also be governed by large scale meteorological phenomena.

The observation of sea-ice motion is important in its response to external atmospheric forcing and the consequent changes in ice-water concentration which, in turn, have a direct effect on shelf water formation, though how this is related to the actual production signal is uncertain.

Acknowledgements

The authors gratefully acknowledge the support of the UK Natural Environment Research Council (grant GR3/6734) and the Geoscience Division of the British Antarctic Survey (BAS) under whose auspices the research was conducted. The Alfred Wegener Institut, Bremerhaven, enabled deployment of drifter 5346. Thanks to Professor Ted Foster of the University of Southern California at Santa Cruz for invaluable discussion, encouragement and computer software and to colleagues at BAS both onshore and off. Peter Wadhams at the Scott Polar Research Institute also supported this work.

References

BAKER, J., NOWLIN, W.D., PILLSBURY, R.D. & BRYDEN, H.L. 1977. Antarctic Circumpolar Current: space and time fluctuations in the Drake Passage. *Nature*, **268**, 696-699.

BRITISH ANTARCTIC SURVEY 1985. *Tectonic map of the Scotia arc*, 1:3000000, BAS (Misc) 3, Cambridge: British Antarctic Survey, 1985.

BRYDEN, H.L. 1979. Poleward heat flux and conversion of available potential energy in the Drake Passage. *Journal of Marine Research*, **37**, 1-22.

CARLETON, A.M. 1988. Sea ice atmosphere signal of the Southern Oscillation in the Weddell Sea, Antarctica. *Journal of Climate*, **1**, 379-388.

CRANE, D.R. & BULL, D. 1990. The Weddell ice dynamics experiment. *Report 90-2, Sea Ice Group, Scott Polar Research Institute, University of Cambridge, England.* [Unpublished manuscript]

DEACON, G.R. & MOOREY, J.A. 1975. The boundary region between currents from the Weddell Sea and Drake Passage. *Deep-Sea Research*, **22**, 265-268.

DEACON, G.R. & FOSTER, T.D. 1976. The boundary region between the Weddell Sea and Drake Passage currents. *Deep-Sea Research*, **24**, 505-510.

FAHRBACH, E., KNOCHE, M. & ROHARDT, G. 1991. An estimate of water mass transformation in the southern Weddell Sea. *In* TREGUER,P. & QUEGUINER, B. *eds. Biochemistry and Circulation of Water Masses in the Southern Ocean. Marine Chemistry*, **35**, Special Issue, 25-44.

FOLDVIK, A., GAMMELSROED, T. & TORRESEN, T. 1985. Circulation and water masses on the Southern Weddell Sea Shelf. *Antarctic Research Series*, **43**, 5-20.

FOLDVIK, A. & KVINGE, T. 1974. Bottom currents in the Weddell Sea. *Report 37, Geophysical Institute, University of Bergen, Norway.*

FOLDVIK, A., MIDDLETON, J.H. & FOSTER, T.D. 1990. The tides of the southern Weddell Sea. *Deep-Sea Research*, **37**, 1345-1362.

FOSTER, T.D. & CARMACK, E.C. 1976. Frontal zone mixing and Antarctic Bottom Water formation in the southern Weddell Sea. *Deep-Sea Research*, **23**, 301-317.

FOSTER, T.D., FOLDVIK, A. & MIDDLETON, J.H. 1987. Mixing and bottom water formation in the shelf break region of the southern Weddell Sea. *Deep-Sea Research*, **34**, 1771-1794.

FOSTER, T.D. & MIDDLETON, J.H. 1979. Variability in the bottom water of the Weddell Sea. *Deep-Sea Research*, **26A**, 743-762.

FOSTER, T.D. & MIDDLETON, J.H. 1980. Bottom water formation in the Western Weddell Sea. *Deep-Sea Research*, **27A**, 367-381.

FOSTER, T.D. & MIDDLETON, J.H. 1984. The oceanographic structure of the Eastern Scotia Sea. I-Physical Oceanography. *Deep-Sea Research*, **31**, 529-550.

GILL, A.E. 1973. Circulation and bottom water production in the Weddell Sea. Deep-Sea Research, **20**, 111-140.

GORDON, A.L. 1981. Seasonality of Southern Ocean sea ice. *Journal of Geophysical Research*, **86**, 4193-4197.

HIBLER, W.D.III, & ACKLEY, S.F. 1983. Numerical simulation of the Weddell Sea pack ice. *Journal of Geophysical Research*, **88**, 2873-2887.

HUTHNANCE, J.M. 1983. Simple models for Atlantic diurnal tides. *Deep-Sea Research*, **30**, 15-29.

IRISH, J.D. & SNODGRASS, F.E. 1972. Australian-Antarctic Tides. *Antarctic Research Series*, **19**, 101-116.

JENKINS, A. 1992. *Dynamics of Ronne Ice Shelf and its interaction with the ocean.* Ph.D thesis, Council for National Academic Awards, [Unpublished].

JENKINS, A. & DOAKE, C.S.M. 1991. Ice-Ocean interaction on Ronne Ice Shelf, Antarctica. *Journal of Geophysical Research*, **96**, 791-813.

LEMKE, P., TRINKL, W. & HASSELMANN, K. 1980. Stochastic dynamic analysis of polar sea ice variability. *Journal of Physical Oceanography*, **10**, 2100-2120.

MASSOM, R.A. 1992. Observing the advection of sea ice in the Weddell Sea using buoy and satellite passive microwave data. *Journal of Geophysical Research*, **97**, 15559-15572.

MCPHEE, M.G. 1978. A simulation of inertial oscillation in drifting pack ice. *Dynamics of Atmospheres and Oceans*, **2**, 107-122.

MIDDLETON, J.H. & FOSTER, T.D. 1977. Tidal currents in the central Weddell Sea. *Deep-Sea Research*, **24**, 1195-1202.

NOWLIN, W.D. JR & ZENK, W. 1988. Westward bottom currents along the margin of the South Shetland Island Arc. *Deep-Sea Research*, **35**, 269-301.

ORSI, A.H, NOWLIN, W.D. JR & WHITWORTH, T. III 1993. On the circulation and stratification of the Weddell Gyre. *Deep-Sea Research*, **40**, 169-203.

PATTERSON, S.L. & SIEVERS, H.A. 1980. The Weddell-Scotia confluence. *Journal of Physical Oceanography*, **10**, 1584-1610.

PILLSBURY, R.D., WHITWORTH, T., NOWLIN, W.D. & SCIREMAMMANO, F. 1979. Currents and temperatures as observed in the Drake Passage during 1975. *Journal of Physical Oceanography*, **9**, 470-482.

PUDSEY, C.J., BARKER, P.F. & HAMILTON, N. 1988. Weddell Sea abyssal sediments: a record of Antarctic Bottom Water flow. *Marine Geology*, **81**, 289-314.

ROWE, M.A., SEAR, C.B., MORRISON, S.J., WADHAMS, P., LIMBERT, D.W.S. & CRANE, D.R. 1989. Periodic motions in Weddell Sea pack ice. *Annals of Glaciology*, **12**, 145-151.

SARUKHANYAN, E'.I. 1980. *Structure and variability of the Antarctic Circumpolar Current* [In Russian]. Leningrad: Hydrometeorological Service, 108pp.

SCHWIDERSKI, E.W. 1981. *Global ocean tides. I-IV. Atlas of tidal charts and maps.* Virginia: Naval Surface Weapons Center Reports TR 81-142/4, Dahlgren, Virginia.

WEBSTER, F. 1968. Observations of inertial period motions in the deep sea. *Reviews of Geophysics*, **6**, 473-490.

WHITWORTH, T.III & NOWLIN, W. 1987. Water masses and currents of the Southern Ocean. *Journal of Geophysical Research*, **92**, 6463-6476.

ZWALLY, H.J., PARKINSON, C.L. & COMISO, J.C. 1983. Variability of Antarctic sea ice and changes in carbon dioxide. *Science*, **220**, 1005-1012.

ZWALLY, H.J., PARKINSON, C.L., CARSEY, F., GLOERSEN, P., CAMPBELL, W.J. & RAMSEIER, R.O. 1979. Antarctic sea ice variations 1973–75. *NASA Weather Climate Review*, **56**, 335-340.